Supplementary Information

Photo-Switchable Phosphotungstic Acid Active Sites in Metal-Organic Frameworks for Tailorable Deacetalization Reaction

*Hui Wen[1], Guoliang Liu[1], Shi-Chao Qi, Chen Gu, Tao Yang, Peng Tan and Lin-Bing Sun**

State Key Laboratory of Materials-Oriented Chemical Engineering, Jiangsu National Synergetic Innovation Center for Advanced Materials (SICAM), College of Chemical Engineering, Nanjing Tech University, Nanjing 211816, China. Corresponding author: lbsun@njtech.edu.cn.

EXPERIMENTAL DETAILS

Chemicals

Chromium (III) nitrate nonahydrate ($Cr(NO_3)_3 \cdot 9H_2O$, Sigma-Aldrich, ≥99 %), 2-nitroterephthalic acid (H_2-NO_2-BDC, Sigma-Aldrich, ≥99 %), hydrofluoric acid (HF, Sigma-Aldrich, 48-51 %), hydrochloric acid (HCl, Sigma-Aldrich, 36-38 %), methanol (MeOH, Sinopharm, ≥99 %), ammonium fluoride (NH_4F, Greagent, ≥98 %), stannous chloride dihydrate ($SnCl_2 \cdot 2H_2O$, Adamas-Beta, ≥99 %), acetonitrile (MeCN, Sigma-Aldrich, ≥ 99%), phosphotungstic acid hydrate (PTA, Adamas-Beta, ≥99 %), *p*-phenylazobenzoylchloride (PAC, TCI, ≥98 %), and benzaldehyde dimethyl acetal (Adamas-Beta, ≥98 %) were commercial chemicals. Deionized water was generated by a Milli-Q integral pure and ultrapure water purification system and used in all experiments.

Materials Synthesis

Preparation of Cr-MIL-101-NO_2 (MOF-NO_2). MOF-NO_2 was synthesized hydrothermally by following the reported methods.[1, 2] 433 mg $Cr(NO_3)_3 \cdot 9H_2O$, 229 mg 2-nitroterephthalic acid, 30 μL HF, and 5 mL deionized water were dissolved and briefly homogenized by sonication. The obtained solution was transferred into a Teflon-lined stainless steel autoclave and kept in oven at 200 °C for 8 h. The as-synthesized green powder was separated from water via filtration and repeatedly washed with deionized water and ethanol for several times. The obtained green powder was further purified in alcohol aqueous solution at 80 °C for 24 h to remove residual ligand. 100 mg crude sample and 17 mg NH_4F were added into a round bottom flask containing 15 mL deionized water. The mixture after sonication was stirred at 60 °C for 12 h, and then repeatedly washed with hot water and ethanol. The obtain powder was dried under vacuum to acquire MOF-NO_2 (180 mg).

Preparation of Cr-MIL-101-NH_2 (MOF-NH_2). The MOF-NH_2 was synthesized by stirring 100 mg MOF-NO_2 and 700 mg $SnCl_2 \cdot 2H_2O$ in 30 mL ethanol at 80 °C for 6 h. When the mixture was cooled to room temperature, the ethanol was removed by centrifugation. 10 mL concentrated HCl were added and the reaction mixture was centrifuged. Finally, the obtained solid was washed several times with water and ethanol and dried.[3, 4]

Materials Characterization

X-ray diffraction (XRD) patterns of materials were recorded using a Bruker D8 Advance diffractometer with monochromatic Cu Kα radiation in the 2θ range from 2° to 20° and 40 mA. The N_2 adsorption-desorption isotherms were measured by BELSORP-MAX analyzer at -196 °C, and samples were degassed at 80 °C for 6 h prior to analysis, and the total pore volume was determined from the amount adsorbed at the relative pressure of 0.99. The inductive coupled plasma emission spectrometer (ICP) was recorded in thermo fisher iCAP PRO. Fourier transform infrared (FT-IR) spectra of the samples diluted with KBr in a good proportion of 1:150, and carried out on a Thermo Nicolet iS10 spectrometer. SEM images and SEM-mapping analyses were collected on a Hitachi S4800 field emission scanning electron microscope. Solid-state ^{31}P spectra was recorded on an Agilent 600 DD2 spectrometer (Agilent, USA, magnetic field strength 14.1 T) at resonance frequency of 150.72 MHz for ^{31}P using the cross-polarization (CP), magic-angle spinning (MAS), and a high-power 1H decoupling. TEM images and EDX-mapping analyses were measured with Hitachi S4800 field emission transmission electron microscope. Thermo gravimetric analysis (TGA) was tested on a thermobalance (STA-499C, Netzsch). 5 mg of sample was heated from the room temperature to 800 °C at the rate of 10 °C·min^{-1} in the flow of N_2 (20 mL·min^{-1}). The elemental analysis (C, H, and N) was recorded on a Vario Micro Cube elemental analyzer (Elementar Analysensysteme GmbH, Hanau, Germany). UV-Vis spectra were collected on the PerkinElmer Lam2a 35 in the region of 280-600 nm, and the absorption curves of different samples were measured. With the absorption peak of 326 nm as the reference wavelength, the photo-responsive cyclic properties of the samples were measured under alternative UV- and Vis-light irradiation.

Table S1. Textual properties and elemental composition of MOF-NH_2, PMOF-NH_2, PTA(1)@PMOF-NH_2, PTA(2)@PMOF-NH_2, PTA(3)@PMOF-NH_2 and PTA.

Sample	S_{BET}[a]	V_p[b]	Elemental composition (wt %)				Loading of
	(m^2 g^{-1})	(cm^3 g^{-1})	C	N	H	P	PTA[c] (wt %)
MOF-NH_2	2695	2.03	36.62	3.84	5.67	–	–
PMOF-NH_2	1853	1.38	40.56	5.67	5.70	–	–
PTA(1)@PMOF-NH_2	893	0.74	14.32	1.84	5.04	0.54	49.0
PTA(2)@PMOF-NH_2	772	0.67	11.33	1.39	3.82	0.60	54.6
PTA(3)@PMOF-NH_2	622	0.50	10.36	1.23	3.11	0.62	56.0
PTA	–	–	0.08	0.01	0.88	–	–

[a] S_{BET} = BET surface area. [b] V_p = pore volume. [c] Measured by ICP.

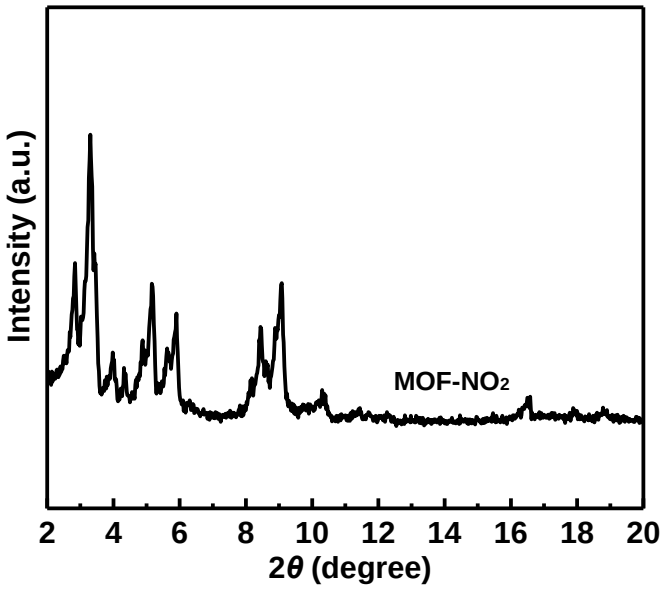

Fig. S1. The XRD pattern of the sample MOF-NO_2.

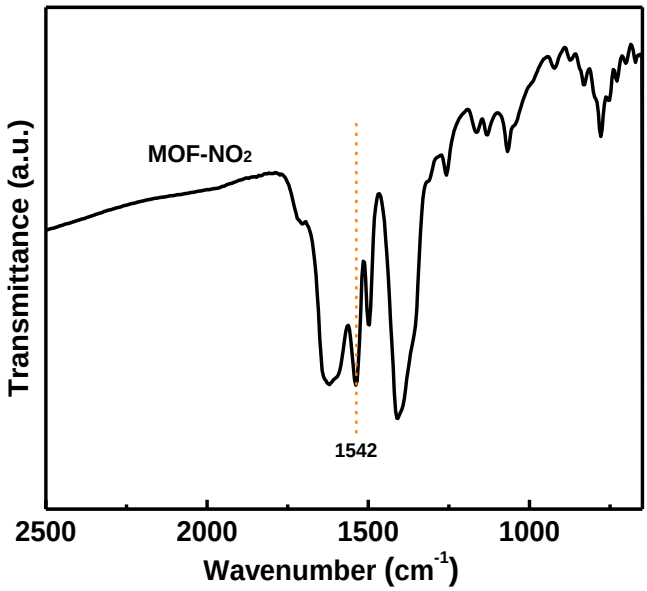

Fig. S2. The FT-IR spectrum of the sample MOF-NO_2.

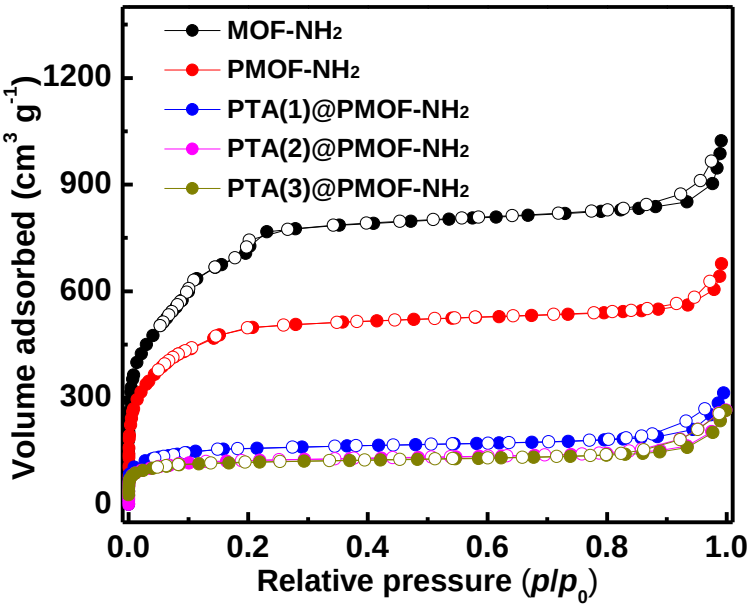

Fig. S3. N_2 adsorption-desorption isotherms of MOF-NH_2, PMOF-NH_2, PTA(1)@PMOF-NH_2, PTA(2)@PMOF-NH_2 and PTA(3)@PMOF-NH_2.

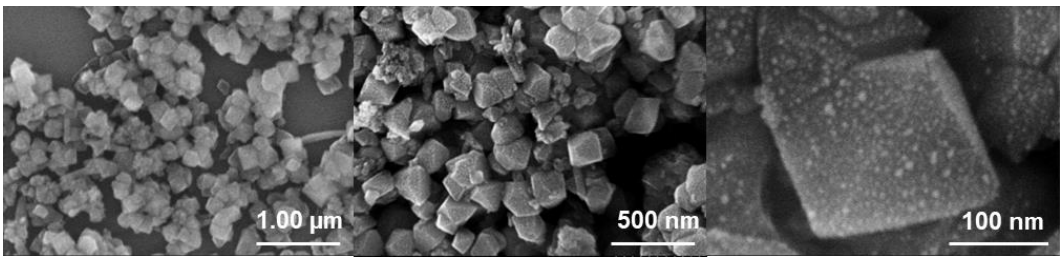

Fig. S4. SEM images of MOF-NH_2 at different magnifications.

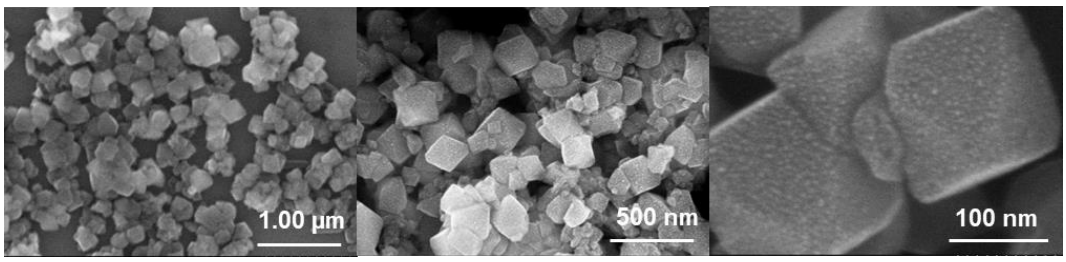

Fig. S5. SEM images of PTA(2)@PMOF-NH_2 at different magnifications.

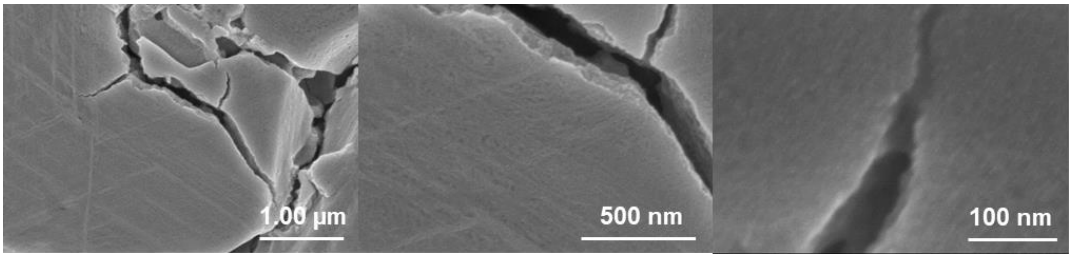

Fig. S6. SEM images of PTA at different magnifications.

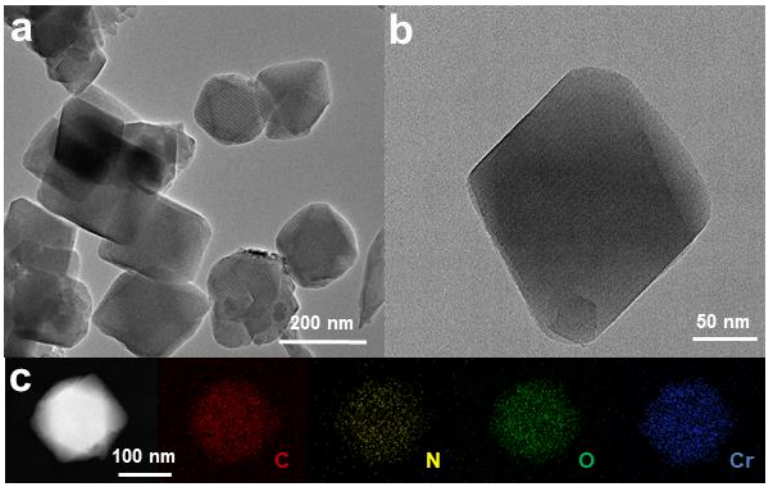

Fig. S7. (a, b) TEM images of and (c) elemental mapping images of the sample MOF-NH_2.

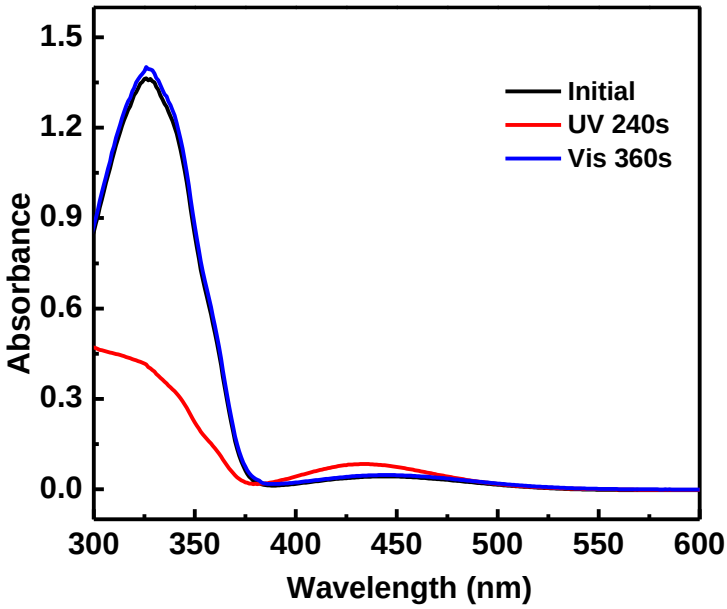

Fig. S8. UV-Vis spectra of PAC after UV- and Vis-light irradiation.

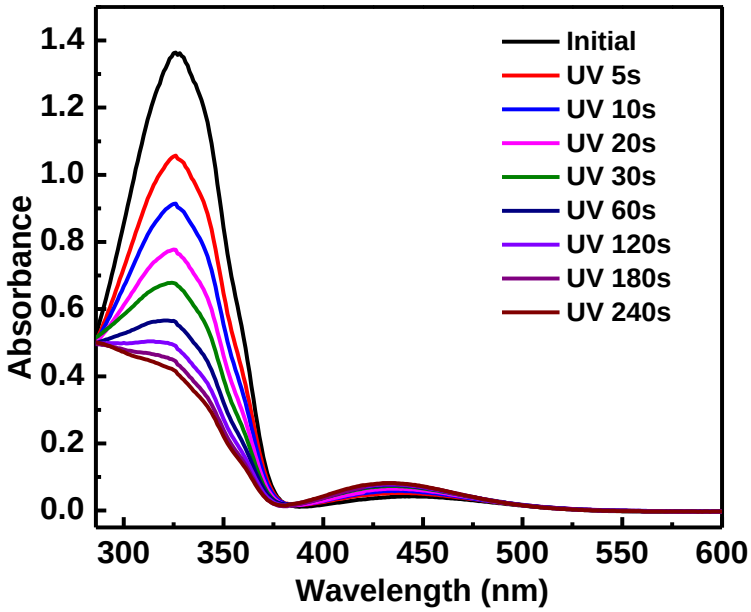

Fig. S9. UV-Vis spectra of PAC after UV-light irradiation.

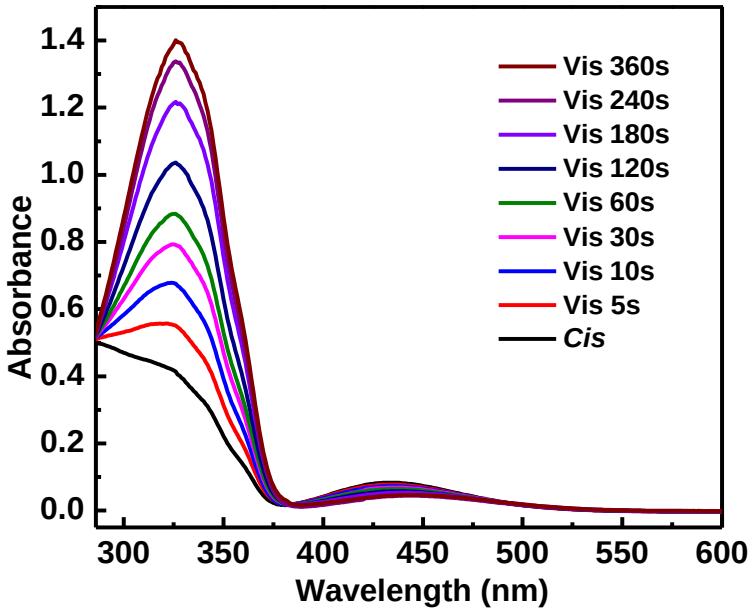

Fig. S10. UV-Vis spectra of PAC after Vis-light irradiation.

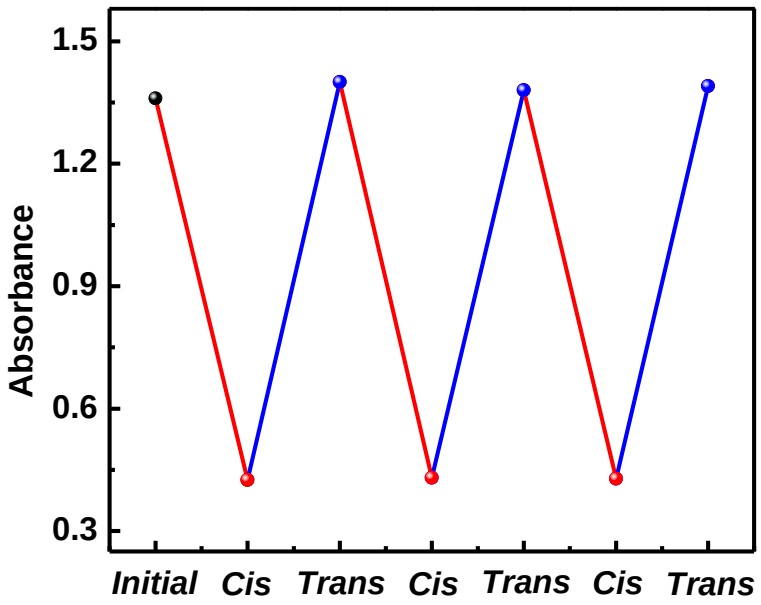

Fig. S11. Reversible change of PAC in absorbance at 326 nm as a function of cycle upon alternating UV- and Vis-light irradiation.

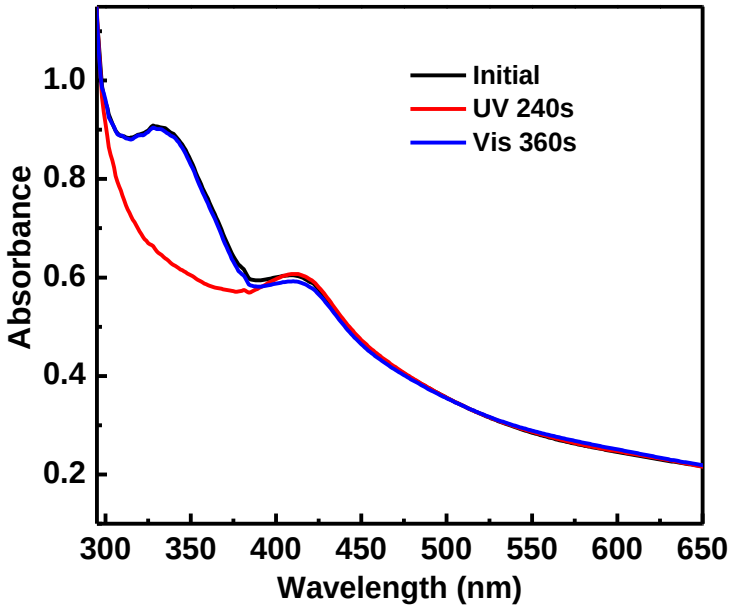

Fig. S12. UV-Vis spectra of PMOF-NH_2 after UV- and Vis-light irradiation.

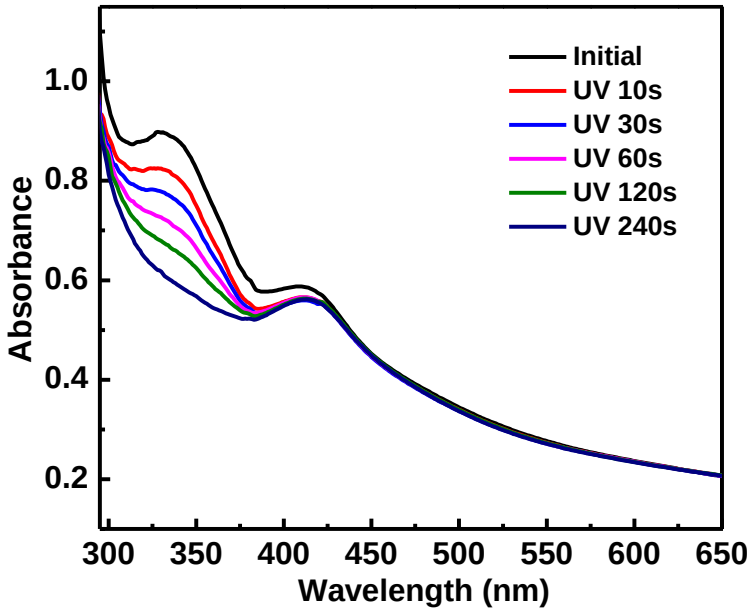

Fig. S13. UV-Vis spectra of PMOF-NH_2 after UV-light irradiation.

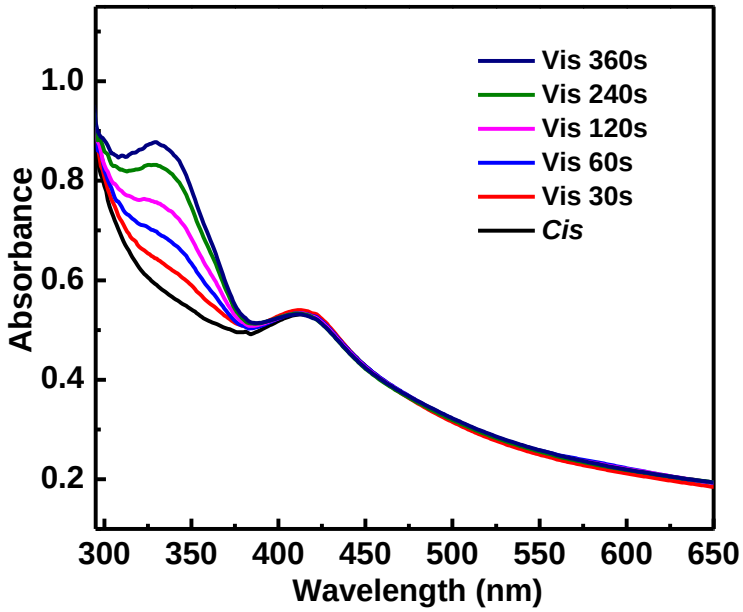

Fig. S14. UV-Vis spectra of PMOF-NH_2 after Vis-light irradiation.

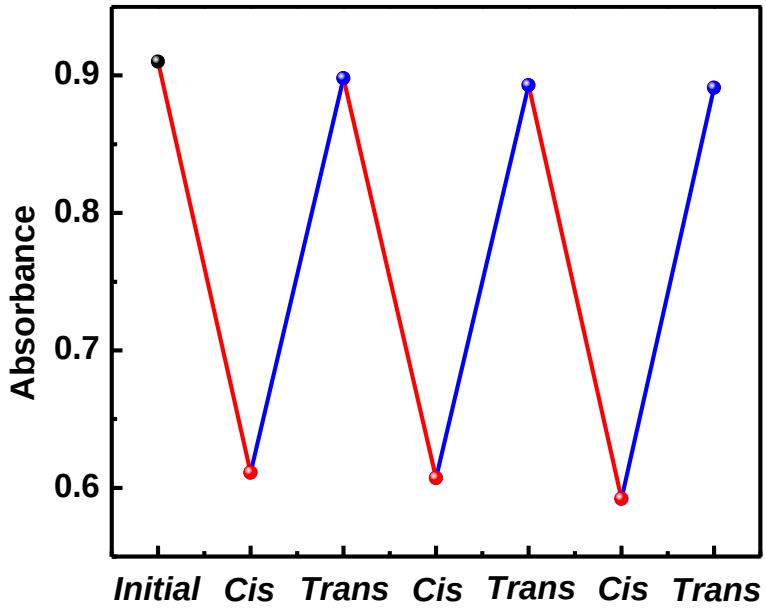

Fig. S15. Reversible change of PMOF-NH_2 in absorbance at 326 nm as a function of cycle upon alternating UV- and Vis-light irradiation.

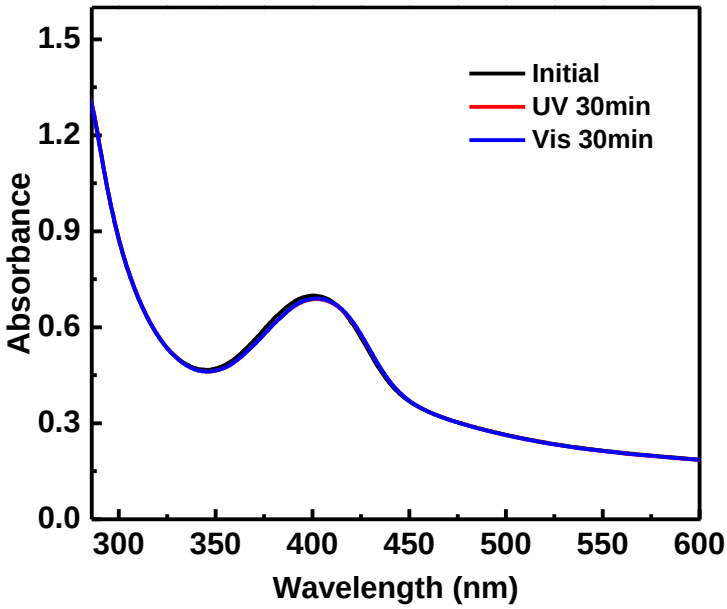

Fig. S16. UV-Vis spectra of MOF-NH_2 after UV- and Vis-light irradiation.

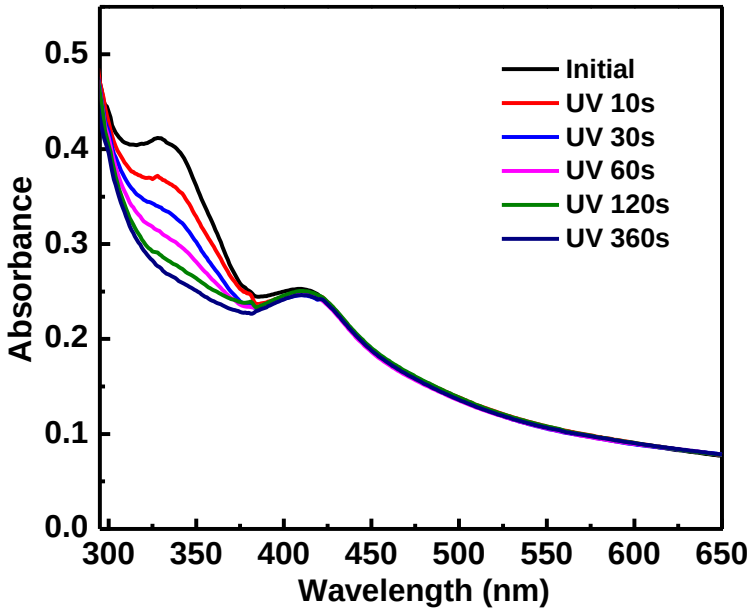

Fig. S17. UV-Vis spectra of PTA(2)@PMOF-NH_2 after UV-light irradiation.

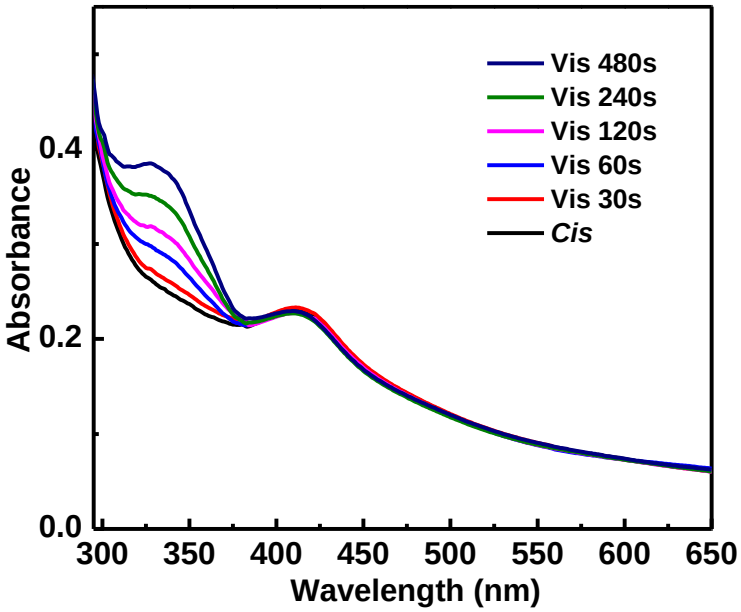

Fig. S18. UV-Vis spectra of PTA(2)@PMOF-NH_2 after Vis-light irradiation.

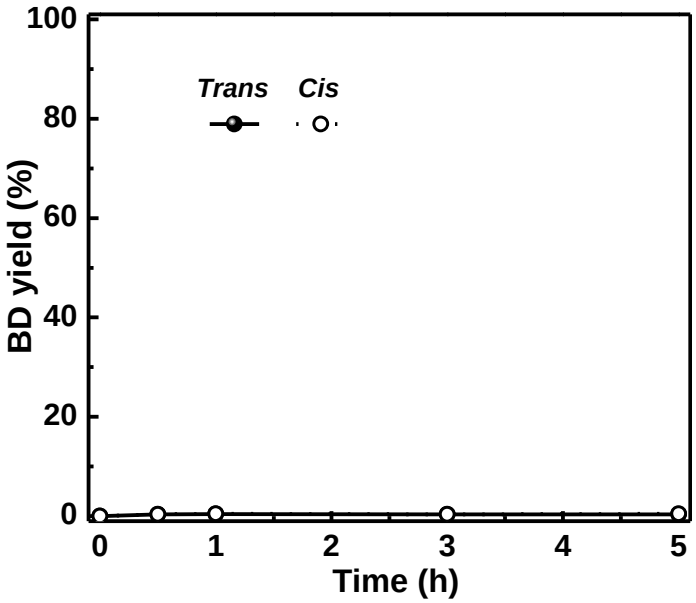

Fig. S19. The catalytic performance of PAC after UV- and Vis-light irradiation.

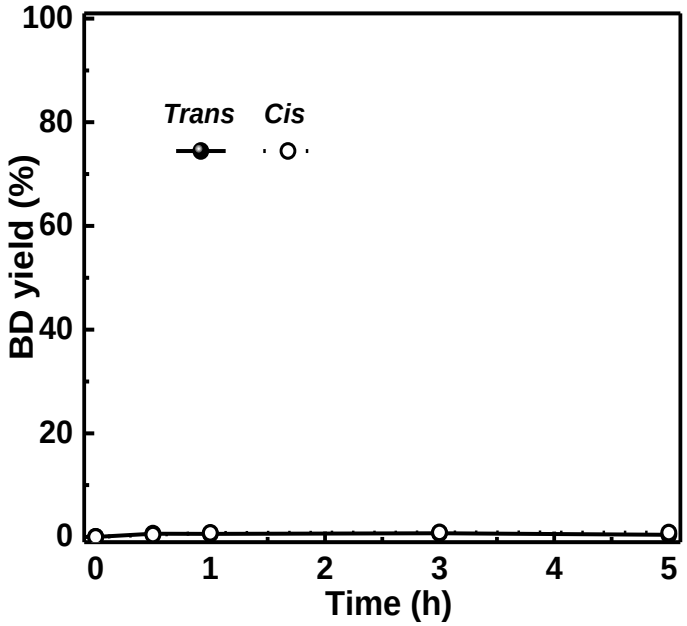

Fig. S20. The catalytic performance of MOF-NH_2 after UV- and Vis-light irradiation.

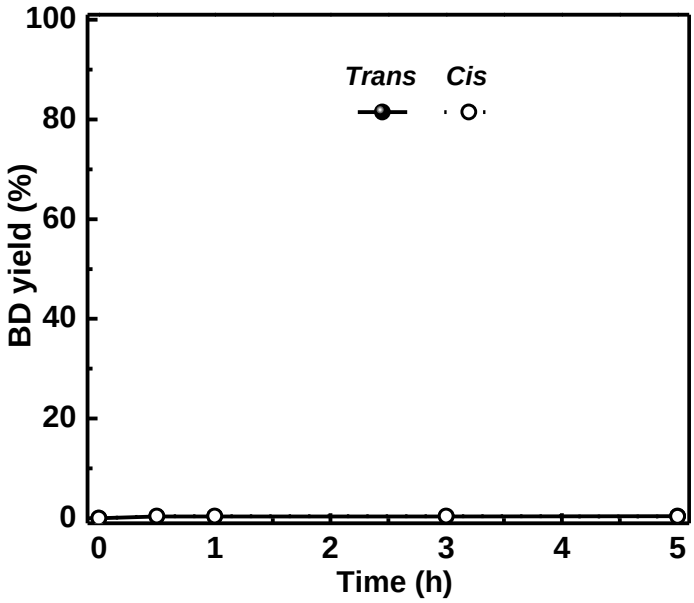

Fig. S21. The catalytic performance of PMOF-NH_2 after UV- and Vis-light irradiation.

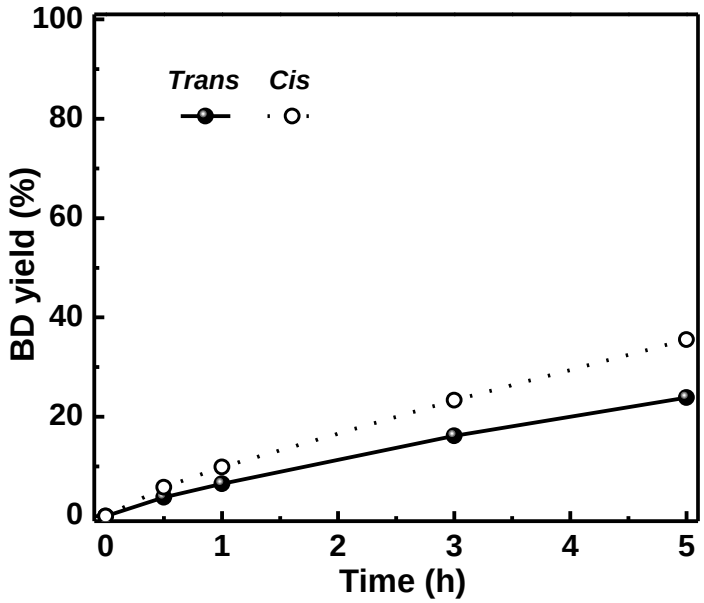

Fig. S22. The catalytic performance of PTA(1)@PMOF-NH_2 after UV- and Vis-light irradiation.

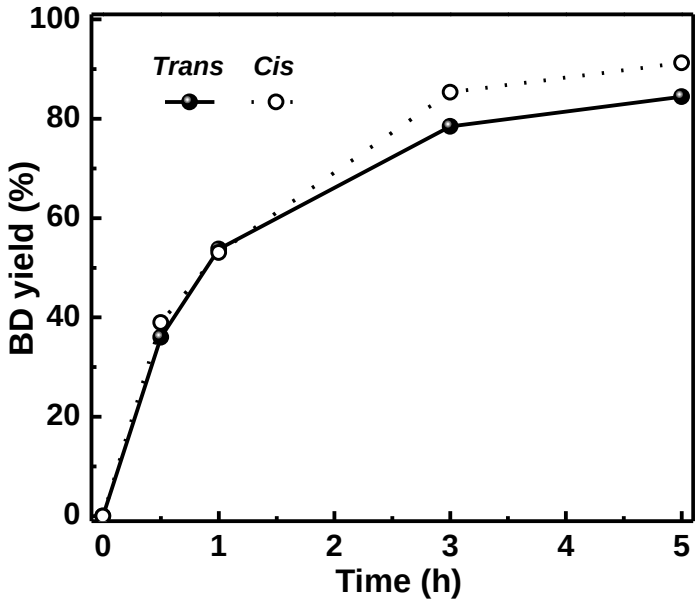

Fig. S23. The catalytic performance of PTA(3)@PMOF-NH_2 in UV- and Vis-light irradiation.

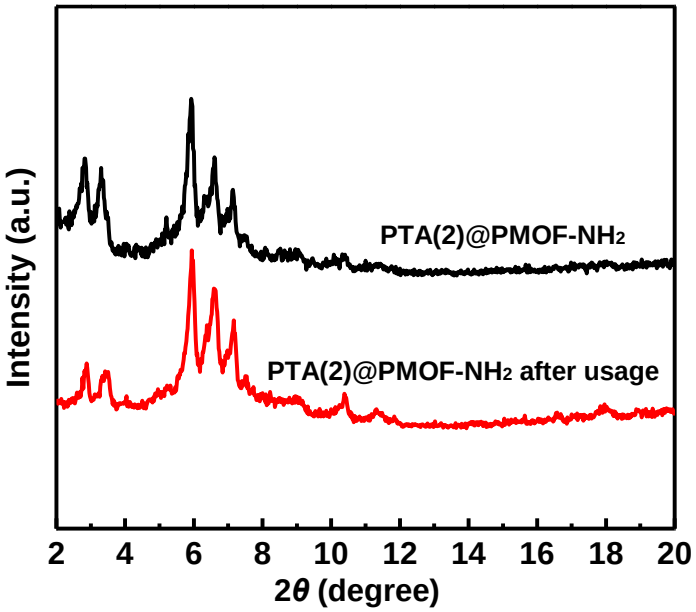

Fig. S24. The XRD patterns of PTA(2)@PMOF-NH_2 before and after usage.

REFERENCES

1. B. Li, Y. Zhang, D. Ma, L. Li, G. Li, G. Li, Z. Shi and S. Feng, *Chem. Commun.*, 2012, **48**, 6151-6153.
2. A. Modrow, D. Zargarani, R. Herges and N. Stock, *Dalton. Trans.*, 2012, **41**, 8690-8696.
3. X. Gao, Y. Ding, Y. D. Sheng, M. C. Hu, Q. G. Zhai, S. N. Li, Y. C. Jiang and Y. Chen, *ChemCatChem*, 2019, **11**, 2828-2836.
4. X. Zhao, K. Wang, Z. Gao, H. Gao, Z. Xie, X. Du and H. Huang, *Ind. Eng. Chem. Res.*, 2017, **56**, 4496-4501.